Huang Ru (Orcid ID: 0000-0002-5124-1950)
Zhang Baoqing (Orcid ID: 0000-0001-6198-6633)
Zhu Haifeng (Orcid ID: 0000-0001-9968-7284)
Liang Eryuan (Orcid ID: 0000-0002-8003-4264)

Spring hydroclimate reconstruction on the south-central Tibetan Plateau inferred from *Juniperus pingii* var. *wilsonii* shrub rings since 1605

Xiaoming Lu[1], Ru Huang[1], Yafeng Wang[2], Baoqing Zhang[3], Haifeng Zhu[1,4], J Julio Camarero[5], and Eryuan Liang[1,4]

[1]Key Laboratory of Alpine Ecology, Institute of Tibetan Plateau Research, Chinese Academy of Sciences, Beijing 100101, China, [2]College of Biology and the Environment, Nanjing Forestry University, Nanjing 210037, China, [3]Key Laboratory of Western China's Environmental Systems (Ministry of Education), College of Earth and Environmental Sciences, Lanzhou University, Gansu, China, [4]CAS Center for Excellence in Tibetan Plateau Earth Sciences, Beijing 100101, China, [5]Instituto Pirenaico de Ecología (IPE-CSIC), Avda. Montañana, 1005, 50059 Zaragoza, Spain

Correspondence to: Eryuan Liang, liangey@itpcas.ac.cn

Key points:

Long-lived alpine Wilson juniper shrubs provide a rare opportunity to retrieve past hydroclimate changes in treeless areas.

Dwarf juniper shrub rings above 4740 m a.s.l. were used to reconstruct 406-year hydroclimate variability on the central Tibetan Plateau.

Little Ice Age was characterized by two long-term dry periods (1637–1683 and 1708–1785).

This article has been accepted for publication and undergone full peer review but has not been through the copyediting, typesetting, pagination and proofreading process which may lead to differences between this version and the Version of Record. Please cite this article as doi: 10.1029/2020GL087707

Abstract Alpine regions on the Tibetan Plateau are sensitive to climate change, however, little is known about their long-term hydroclimate variability due to short and few instrumental records. Alpine shrub provides a rare opportunity to reconstruct past high-resolution hydroclimate conditions. Here, we used living and dead juniper shrubs (*Juniperus pingii* var. *wilsonii*) to develop a 537-year ring width chronology nearby the Nam Co Lake (4725 m a.s.l.). The chronology explained 46% of variance in May-June Standardized Moisture Anomaly Index (SZI) in the period from 1970 to 2010. We reconstructed May-June SZI since 1605. The reconstructed SZI matched well with several tree-ring based moisture or drought reconstructions for the Tibetan Plateau region. In particular, two long dry May-June periods of 1637–1683 and 1708–1785 during the Little Ice Age (LIA) implied that long-term cold temperature tends to slow down hydrological cycle in the margin areas of the Indian summer monsoon.

Plain Language Summary As the Third Pole, the Tibetan Plateau is a core region for global change studies given that it is warming at twice the global average rate. The central Tibetan Plateau with an elevation above 4500 m a.s.l. is characterized by extremely cold and dry treeless environment. However, very few alpine shrub species there provide a rare opportunity to retrieve changes of alpine ecosystem by shrub-ring analysis. In spite of their small basal diameters (mean of 12 cm), we established a 537-year standard shrub ring chronology by crossdating living and dead Wilson juniper shrubs sampled above 4740 m a.s.l. on the central Tibetan Plateau. It is, to date, one of the world's longest shrub-ring chronologies. Shrub-ring chronology from 1605 to 2010 was then used to reconstruct mean May-June drought severity (Standardized Moisture Anomaly Index). Two long-term dry spring periods (1637–1683 and 1708–1785) occurred during the Little Ice Age (LIA), implying that cold temperature slows down hydrological cycle. This study highlights the importance of alpine juniper shrubs in understanding hydrological cycle in dry, continental alpine treeless areas.

1. Introduction

As the "Water Tower of Asia", the Tibetan Plateau is undergoing rapid changes such as cryospheric melt (Yao et al., 2019) and greening of alpine ecosystems (Piao et al., 2020) because climate warming there is faster than at the low altitude regions in recent decades. However, short-term instrumental records, and particularly hydroclimate records, impede a better understanding on ecological and environmental processes prior to the 1950s on the Tibetan Plateau. Thus, climate proxies such as tree rings (Cook et al., 2010), ice (Yao et al., 2019) and lake sediment cores (Zhu et al., 2015) have been used to reconstruct past climate in this region. Among these proxies, tree rings play an important role in retrieving past climatic change from century to millennia time scales on the Tibetan Plateau (Fang et al., 2010; Gou et al., 2015; Liu et al., 2019; Shao et al., 2010; Yang et al., 2019; Zhang, Evans, et al., 2015).

Trees are absent at high-elevation areas (i.e., generally above 4400 m a.s.l.) on the south-central Tibetan Plateau, where patches of alpine shrub species can survive. As in the case of trees, shrubs form annual growth rings that record climatic influences (Liang et al., 2012; Schweingruber & Poschlod, 2005; Xiao et al., 2019). Some alpine shrub species are long lived (> 1000 years), thereby extending far beyond the instrumental climate records (Camarero & Ortega-Martínez, 2019). Shrub-ring width can therefore provide a unique opportunity to reconstruct past climate conditions in alpine treeless areas and allow assessing how recent climate change impacts those areas.

Among alpine shrubs, Wilson juniper (*Juniperus pingii* var. *wilsonii*) is widespread throughout the south-central Tibetan Plateau, and its radial growth depends largely on moisture availability in current May-June and previous September (Liang et al., 2012). Moreover, shrub-ring $\delta^{18}O$ of Wilson juniper was also strongly and negatively linked to air moisture (Wernicke et al., 2019). Wilson juniper is therefore one of the most suitable shrub species to reconstruct drought history in alpine areas over the south-central Tibetan Plateau. Drought associated with climate change in recent decades has serious agricultural and social-economic effects on the southern Tibetan Plateau (Chen, Liu, et al., 2019). Long-term and high resolution drought records are, however, scarce for this region, preventing a better understanding on past drought history.

Regional climates on the south-central Tibetan Plateau (30°–35° N) are influenced by the interactions between the Indian summer monsoon and westerlies (Chen, Chen, et al., 2019; Zhu et al., 2015). The Nam Co, situated within this transitional region, is located at the northernmost limit of distribution of Wilson juniper on the Tibetan Plateau. The objectives of this study are: (i) to establish a long, well-replicated, regional shrub-ring chronology from living and dead juniper shrubs in the Nam Co region, and (ii) to reconstruct past regional hydroclimate conditions. Additionally, based on a study indicating that water level of Nam Co was low in the Little Ice Age (LIA) (Wrozyna et al., 2010), we hypothesized that the cold LIA was characterized by dry periods.

2. Methods

2.1 Study site and climate

The Nam Co Lake (30.5°–30.89° N, 90.27°–91.05° E, 4725 m a.s.l.) is located at the northern flank of the Gangdise-Nyainqentanglha Mountains (Zhu et al., 2015). The vegetation surrounding the lake consists of the alpine steppes and dwarf juniper shrublands. The study was carried out at the northern shore of the Nam Co Lake (Figure 1, 30.88° N, 90.87° E; 4740–4800 m a.s.l.).

Climate in the Nam Co region is characterized by semi-arid to semi-humid alpine conditions. The meteorological station at Baingoin (4700 m a.s.l.) is situated at about 100 km north-west of the Nam Co Lake. During the period of 1957–2013, the mean temperatures in January and July at Baingoin station were −11.29 °C and 9.07 °C, respectively. The mean annual precipitation was 316 mm (Liang et al., 2012). Snowfall usually occurs in this region from October of the previous year to June of the current year. Such snow-related conditions (e.g., snow depth) may have great influence on moisture variability. Self-calibrating Palmer Drought Severity Index (PDSI) was used to quantify the drought severity for the target region at a given time (Wells et al., 2004). Standardized Precipitation Evapotranspiration Index (SPEI) was based on water balance which includes both precipitation and temperature effects (Vicente-Serrano et al., 2010). It allows characterizing drought at different time scales (1–48 months). In comparison with PDSI and SPEI, the Standardized Moisture Anomaly Index (SZI)

is based on water budget simulations, and incorporates effects of snow dynamics on soil moisture availability. It also captures the duration and severity of multiyear droughts through its multi-scalar feature at varied spatial scales. This is crucial for quantifying drought events in the study alpine tundra areas with long lasting snow cover period (Zhang, Zhao, et al., 2015; Zhang et al., 2019). Thus, the SZI instead of other drought indices (e.g., PDSI; SPEI) was selected for drought reconstruction. In this study, the considered analysis period was 1970–2010 for the region limited by coordinates 30.75°–34.50° N and 90.00°–91.00° E.

2.2 Dendrochronological methods

In August 2010, 33 Wilson juniper discs were sampled around the northern shore of the Nam Co Lake. These samples are well dated and continuous missing rings have not been detected when we applied series-section method at multiple points along two whole stems (Liang et al., 2012). In September 2015, additional 3 living and 33 dead juniper shrub remnants were collected either from the area nearby the previous sampling site or the yard of local residents. Among them, 6 dead remnants have a clear sign of wood rot at outer part of the stems. All wood samples were air dried, progressively sanded (100–1200 grits) until rings were clearly visible and visually cross-dated under the stereomicroscope. The ring-widths were then measured under the Lintab 6 system with a resolution of 0.01 mm. One to three radii were measured for each cross-section. The quality of cross-dating was tested in COFECHA and potential occurrence of missing rings was verified (Holmes, 1983). 81% of the dead individuals have a mean age of ca. 245 years and formed their outermost rings during the period of 1969–2014. In total, 69 cross-sections with 125 radii were successfully cross-dated and used in the analyses.

Detrending was performed using ARSTAN program (Cook & Krusic, 2008). Raw ring-width series were first fitted by a straight line of any slope or by 67%-long cubic smooth splines with 50% percent variance cutoff. Then, ring-width indices were obtained by dividing observed by fitted values. A standard ring-width chronology was established by calculating the mean value of the detrended ring-width series by using a bi-weight robust estimation.

Several descriptive statistics of the standard chronology were computed (Cook et al., 1990).

Mean sensitivity (MS) is a measurement of relative difference between the adjacent rings (Fritts, 1976). First-order autocorrelation (AC1) quantifies the relative influence of the growth in previous year to the current year. Mean series inter-correlation among growth curves (Rbar), was calculated within (Rbar.w) and between individuals (Rbar.b). Expressed Population Signal (EPS) and Signal-to-Noise Ratio (SNR) were also calculated to evaluate the reliability and replication of the standard chronology through time (Wigley et al., 1984). Lastly, the first principal component (PC1) was used to quantify how much variance was accounted for by the common pattern of year-to-year growth variability.

2.3 Climate-growth relationships

Pearson correlation analysis was performed to investigate the relationships between the shrub ring-width chronology and monthly moisture/drought variables of precipitation, SZI, PDSI, SPEI and snow depth over the period of 1970–2010. This analysis included a 15-month window extending from July of the previous year to September of the current year. We also calculated the correlation for the cumulative monthly average or sum of May-June climate variables as moisture in that period was considered critical to the juniper shrub growth based on a previous study (Liang et al., 2012). Monthly drought indices of PDSI and SPEI (1-month scale) were downloaded from the KNMI Climate Explorer webpage (https://climexp.knmi.nl/) which is a web-based application containing instrumental and interpolated climate data and allows performing analyses as spatial correlations (Trouet & Oldenborgh, 2013). The Pearson correlations between the first differences of the chronology and above climate variables were calculated to investigate their relationship stability on the inter-annual domain. In addition, we correlated our chronology with SZI at different monthly scales (1 to 48 months). Only the correlations between the chronology and May-June SZI in a 5-month period were shown as the highest correlation coefficients were found for this time scale.

2.4 Climate reconstruction: calibration and verification

A simple linear regression model was employed to reconstruct variations in SZI. The period of 1970–2010 was divided into two almost equal sub-periods (1970–1990 and 1991–2010)

for independently calibration and verification analyses (Cook et al., 1990). A linear regression model was calibrated and verified in both periods. Leave one out procedure using the entire period (1970–2010) was also applied for the validation (Michaelsen, 1987). The reliability of the linear regression models was assessed by commonly used statistics including: the determination coefficient quantifying the explained variance (r^2) and its adjusted version (r^2adj), F value, reduction of error (RE), coefficient of error (CE) (Fritts, 1976). RE and CE play important roles in the calibration and verification procedures. Their values range from negative infinity to one, indicating a perfect estimation (Cook et al., 1990). The non-parametric measures of sign test (ST) and its first differences (FST) were also used to test the reliability of the linear regression models. Product means test (PMT) was used as a diagnostic tool since it considers the signs and similarities of calibration and verification datasets (Fritts, 1976). The reconstruction is analyzed to detect the wet (above average) and dry (below average) periods. Extreme wet and dry years were identified considering one and two standard deviation (SD) thresholds (± 1SD and ± 2SD). The Savitzky and Golay (1964) running mean curve based on a least squares polynomial fitting across 10-year moving window was used to highlight the relative low-frequency variation of the reconstruction.

Our reconstruction was compared with nearby tree-ring based moisture or drought reconstructions at Reting (30.3° N, 91.52° E; ca. 90 km away; Bräuning & Grießinger, 2006) and Zaduo sites (32.66° N, 95.72° E; ca. 490 km away; Shi et al., 2009) (Figure 1). Three PDSI reconstructions that focused on Asia (31.25° N, 91.52° E; ca. 50km away; 0.5°×0.5° grids located near our study site), southern and northern Tibetan Plateau, were also used for comparison (Cook et al., 2010; Zhang, Evans, et al., 2015). Finally, the representation of SZI reconstruction was assessed by using spatial correlation analyses with several hydroclimate datasets. The climate variables include 0.5°-gridded May-June precipitation data of climate research unit (CRU TS 4.03), CRU self-calibrating PDSI and SPEI (1-month scale) drought indices (https://climexp.knmi.nl/) as well as raw SZI dataset (0.25°×0.25° grid, 5-month scale, Zhang et al., 2019) for the period of 1970–2010.

3. Results

3.1 Shrub-ring chronology and related climate signals

We established a 537-year (1479–2015) long Wilson juniper standard shrub ring chronology (Figure S1). Juniper shrubs had a mean ring-width of 0.32 mm (Table S1). The chronology was characterized by moderate MS value (0.29). The low AC1 (0.33) reflected relatively small carry-over effect of the previous year' growth conditions on the shrub growth of current year. EPS values were higher than 0.85 from 1479 onwards, and dropped below the 0.85 threshold during the period 1631–1679 (0.81–0.84) and exceeded 0.85 from 1680 to 2010 (Figure S1). For the common period (1900–2010) analysis, the Rbar was 0.26. Rbar.b was 0.25 whereas Rbar.w equaled 0.58. The variance explained by the PC1 was 28.5%.

Over the period 1970–2010, May and June moisture conditions strongly affected the radial growth of juniper shrub (Figure 2a). Additionally, May-June SZI during the current year (r = 0.677, $p < 0.001$) better predicted juniper shrub growth as well than precipitation (r = 0.572, $p < 0.001$), PDSI (r = 0.517, $p < 0.001$) and SPEI (r = 0.589, $p < 0.001$). Their correlation coefficients were higher (except for precipitation) after removing the first-order autocorrelation of the chronology and moisture indices (Figure 2b). Snowfall in May also had a significant positive effect on juniper growth (Figure S2).

3.2 May-June SZI reconstruction

The split calibration/verification method performed well against the raw May-June SZI data during the independent verified period (Table S2). The chronology explained 41–62% variance of the May-June SZI in two sub-periods (1970–1990 and 1991–2010) and in the full calibration period (1970–2010). As shown by high RE and CE values, the reconstruction provided a reliable estimation of May-June SZI. The May-June SZI reconstruction was finally derived from the linear regression model calculated over the full period (1970–2010) (Figure 2). Concerning the quality and time span of the shrub ring chronology, the reconstructed period covered 406 years with the EPS values close to or above the 0.85 for the period of 1605–2010 (Figure S1).

According to the May to June SZI reconstruction, two long-term dry periods (1637–1683 and

1708–1785) were identified in the low-frequency (10-year moving average) variability (Figure 2d). Over the period of 1786–2010, such low frequency variation of the reconstructed SZI exhibited neither increasing nor decreasing trends with many short wet (e.g., 2000–2005) and dry (e.g., 1904–1917) periods.

Years with extreme dry (62 years; mean−1SD) and wet (55 years; mean+1SD) May-June periods were also detected (Figure 2d). There were 23 extreme dry years in the 17th century, followed by 20th, 18th and 19th centuries with 16, 11 and 11 years, respectively. In contrast, the 17th century included 42% (23 years) of all extreme wet years, whilst the 18th century showed the fewest amount of extreme wet years (6 years). In addition, a total of 26 extreme wet years were determined for the period 1800−2000. These extreme dry and wet periods usually lasted 1 year with some exceptions lasting from 2 to 7 years (e.g., 1820−1821). Of these years, 1640, 1665, 1674, 1676, 1682, 1692, 1715, 1833, 1908, 1914, 1984 and 1995 corresponded to severe droughts (values below mean−2SD). Accordingly, we identified 6 exceptionally wet years (1610, 1611, 1618, 1620, 1702 and 1704; i.e., values above mean+2SD).

Our reconstruction was positively correlated with the ring-width based reconstruction of pre-monsoon (March to May) precipitation at Reting (r = 0.41, 1605–1998, p < 0.001; Figures 1 and 3) developed by Bräuning and Grießinger (2006) and May-June drought index at Zaduo (r = 0.17, 1605–2006, p < 0.001) developed by Shi et al. (2009). It also showed considerable coherence with the 0.5°-gridded reconstruction of the summer PDSI near the sampling site (r = 0.24, 1605–2005, p < 0.001) (Cook et al., 2010) and with May-June PDSI on the southern (r = 0.37, 1605–2006, p < 0.001) and northern (r = 0.15, 1605–2005, p < 0.01) Tibetan Plateau as reconstructed by Zhang, Evans, et al. (2015). Lastly, the spatial correlation preformed for the period of 1970–2010 further indicated that radial growth of juniper shrub growth is representative for Nam Co region hydroclimate (Figure S3).

4. Discussion

There is evidence that snow depth in the early growing season strongly influences juniper shrub growth in study area (Figure S2). However, very few studies have fully considered the

role of snowpack dynamics on soil water and wood plant growth (Belmecheri et al., 2016; Sanmiguel-Vallelado et al., 2019; Zhang et al., 2019). The SZI provides a more reasonable estimation of drought by considering the snow effects on soil moisture and the hydrologic cycle, allowing us to better infer the past hydroclimate variability in the study high-elevation areas.

Juniper shrubs are suitable for long-term hydroclimate reconstructions in alpine ecosystems (Carrer et al., 2019; García-Cervigón et al., 2018). Due to extreme environmental conditions, some juniper shrub species are generally slow-growing and long lived. For example, old living juniper shrubs exceeding 1000 years (^{14}C-dated) have been found in Mediterranean Basin (Camarero & Ortega-Martínez, 2019) and over 840 years old in the Polar Urals (Hantemirov et al., 2004). Alcalá-Reygosa et al. (2018) found juniper shrub patch of 830 years old in Mexico. However, it is still a great challenge to develop long shrub-ring chronologies due to missing or wedging rings. In this study, we found that Wilson juniper can be used to build chronology over 537 years on the southern Tibetan Plateau. We developed, to date, one of the world's longest shrub-ring chronologies in the alpine regions. Considering its wide distribution range, it was possible to build ring-width chronology longer than 600 years on the dry south-central Tibetan Plateau. Assembled Wilson juniper shrub ring chronologies from sites across the Tibetan Plateau will provide an overall and high resolved estimation of alpine hydroclimate variability for the past centuries.

This study revealed that moisture in current early growing season governs drought-prone biomes over the south-central Tibetan Plateau where Wilson juniper shrub is the dominant woody species. It grows on the steep and exposed slopes with shallow, gravel soils, where strong solar radiation and temperature may exacerbate photoinhibition and moisture stress and constrain juniper growth. Shortage of soil moisture in May and June, in combination with increased temperatures, may potentially delay the onset of cambium activity of juniper shrub as has been observed in alpine junipers from semi-arid areas (Ren et al., 2018). Soil moisture compensated from the start of Indian monsoon in mid-May may thus determine the start of the xylogenesis of juniper shrub, which is important to overall radial growth of that species. Recent remote sensing and *in-situ* observation studies also indicate that spring phenology of

alpine grassland is strongly linked to early growing-season precipitation on the southern Tibetan Plateau (Li et al., 2016; Shen et al., 2015). Water stress during the early growing season was also observed at a large spatial scale of forests sites on the Tibetan Plateau and central Himalayas (Liang et al., 2019; Zhang, Evans, et al., 2015). It seems that a high moisture demand during the early growing season is not only limiting growth and productivity in alpine biomes but also in grassland and forests on the Tibetan Plateau. Warming-induced moisture deficit may threaten the sustainability and resilience of ecosystems on the Tibetan Plateau.

Based on May-June drought reconstruction, the Nam Co region was characterized by several long-term dry periods (e.g., 1637–1683 and 1708–1785) during the LIA on the Tibetan Plateau (1430– the late 19th century, Grießinger et al., 2011). In particular, 7 out of the 12 driest years occurred in the 1605–1800 period. Multi-decadal dry springs in the LIA were also recorded by tree rings on the northeastern Tibetan Plateau (Shao et al., 2010; Zhang, Evans, et al., 2015). It implied that cold temperature may slow down hydrological cycle in spring during the LIA. However, high summer precipitation in the period of 1400–1900 (Reting site, Grießinger et al., 2011) and greater annual snow accumulation in 1580–1777 in the Puruogangri ice-cores, located ca. 350 km away from study site (Yao et al., 2008), were observed on the central Tibetan Plateau. Together, the strengthening/weakening of the Indian summer monsoon in early growing season in the LIA could result in wet/dry conditions over the warm/cold periods in its margin areas on the Tibetan Plateau.

As indicated by the spatial correlation analyses, the moisture variability in May-June may be relatively synchronous within the large extent on the southern Tibetan Plateau (Figure S3). Moreover, comparisons between our reconstruction and a set of tree-ring based moisture/drought reconstructions on the Tibetan Plateau also confirm this synchrony in a longer temporal scale (Figure 3). It is important to mention that some reconstructions used for comparison were not limited to May-June months but to specific seasons. For example, pre-monsoon (March to May) rainfall was reconstructed for Reting site (Bräuning & Grießinger, 2006). Despite this limitation, our reconstruction agrees well with nearby tree-ring based drought reconstructions (Bräuning & Grießinger, 2006; Cook et al., 2010; Shi

et al., 2009; Zhang, Evans, et al., 2015), displaying similar variability in selected dry and wet periods (Figures 3a−3d, 3f). In particular, several extreme dry (e.g., 1692, 1693, 1914 and 1995) and wet (e.g., 1790, 1898, 1899 and 1991) years reconstructed in this study agree well with the aforementioned moisture/drought reconstructions. Historical documents on the southern Tibetan Plateau reported a sustained drought during 1907−1915 with great crop failures (Lin & Wu, 1986). This dry period is also corroborated in our reconstruction which revealed a dry period in 1904−1917 with 2 severe drought years in 1908 and 1914. To conclude, the presented alpine juniper shrub ring-width chronology constitutes a reliable hydroclimate proxy for alpine ecosystems on the south-central Tibetan Plateau.

5. Conclusions

We established a long ring-width chronology from living and dead alpine Wilson juniper shrubs around the Nam Co Lake. The shrub-ring chronology explained 46% of the total variance of the May-June SZI over the period of 1970–2010, showing high predictive potential. A 406-year long series of hydroclimate variability was then reconstructed for the south-central Tibetan Plateau. Two long dry periods in 1637–1683 and 1708–1785 were identified during the LIA, supporting the hypothesis that coldest periods correspond to driest situations. In addition, several short-term dry and wet periods agreed well with other moisture/drought reconstructions and historical archives over the southern Tibetan Plateau. Our reconstruction could be further improved by extending the temporal and spatial scale of the sampled high-elevation sites in the future.

Acknowledgments

This work was supported by the Second Tibetan Plateau Scientific Expedition and Research Program (STEP) (2019QZKK0301) and the National Natural Science Foundation of China (41807444, 41525001). We thank the Nam Co Station for Multisphere Observation and Research, Chinese Academy of Sciences for the fieldwork support, and Qi-Bin Zhang for providing May-June PDSI reconstructions on the Tibetan Plateau. Tree-ring data (Zaduo and Reting sites) and gridded PDSI reconstruction data were downloaded from National Oceanic Atmospheric Administration website (https://www.ncdc.noaa.gov/paleo-search/). The

shrub-ring chronology and reconstructed SZI series data are available at National Tibetan Plateau Data Center (https://data.tpdc.ac.cn/en/data/7ff4fcde-4c6a-4e04-bd95-dae4d0d0cbe1/).

References

Alcalá-Reygosa, J., Palacios, D., Schimmelpfennig, I., Vázquez-Selem, L., García-Sancho, L., Franco-Ramos, O., et al. (2018). Dating late Holocene lava flows in Pico de Orizaba (Mexico) by means of *in situ*-produced cosmogenic ^{36}Cl, lichenometry and dendrochronology. *Quaternary Geochronology 47*, 93–106. https://doi.org/10.1016/j.quageo.2018.05.011

Belmecheri, S., Babst, F., Wahl, E. R., Stahle, D. W., & Trouet, V. (2016). Multi-century evaluation of Sierra Nevada snowpack. *Nature Climate Change 6*, 2–3. https://doi.org/10.1038/nclimate2809

Bräuning, A., & Grießinger, J. (2006). Late Holocene variations in monsoon intensity in the Tibetan-Himalayan region-evidence from tree rings. *Journal of the Geological Society of India 68* (3), 485–493.

Camarero, J. J., & Ortega-Martínez, M. (2019). Sancho, the oldest known Iberian shrub. *Dendrochronologia 53*, 32–36. https://doi.org/10.1016/j.dendro.2018.11.003

Carrer, M., Pellizzari, E., Prendin, A. L., Pividori, M., Brunetti, M. (2019). Winter precipitation-not summer temperature-is still the main driver for alpine shrub growth. *Science of the Total Environment 682,* 171–179. https://doi.org/10.1016/j.scitotenv.2019.05.152

Chen, F., Chen, J., Huang, W., Chen, S., Huang, X., Jin, L., et al. (2019). Westerlies Asia and monsoonal Asia: spatiotemporal differences in climate change and possible mechanisms on decadal to sub-orbital timescales. *Earth-Science Reviews 192*, 337–354. https://doi.org/10.1016/j.earscirev.2019.03.005

Chen, Q., Liu, F., Chen, R., Zhao, Z., Zhang, Y., Cui, P., et al. (2019). Trends and risk evolution of drought disasters in Tibet Region, China. *Journal of Geographical Sciences 29* (11), 1859–1875. https://doi.org/10.1007/s11442-019-1993-z

Cook, E., Briffa, K., Shiyatov, S., & Mazepa, V. (1990). Tree-ring standardization and growth-trend estimation. In E. R. Cook, & L. A. Kairiukstis (Eds.), *Methods of dendrochronology: applications in the environmental sciences*. Kluwer Academic, Dordrecht.

Cook, E., & Krusic, P. (2008). A tree-ring standardization program based on detrending and autoregressive time series modeling, with interactive graphics (ARSTAN). Tree-Ring Laboratory, Lamont-Doherty Earth Observatory, Columbia University, Palisades, NY.

Cook, E. R., Anchukaitis, K. J., Buckley, B. M., D'Arrigo, R. D., Jacoby, G. C., & Wright, W. E. (2010). Asian monsoon failure and megadrought during the last millennium. *Science 328* (5977), 486–489. https://doi.org/10.1126/science.1185188

Fang, K., Gou, X., Chen, F., Li, J., D'Arrigo, R., Cook, E., et al. (2010). Reconstructed droughts for the southeastern Tibetan Plateau over the past 568 years and its linkages to the Pacific and Atlantic Ocean climate variability. *Climate Dynamics 35* (4), 577–585. https://doi.org/10.1007/s00382-009-0636-2

Fritts, H. C. (1976). *Tree rings and climate*. Scientific American.

García-Cervigón, A., Linares, J. C., García-Hidalgo, M., Camarero, J. J., & Olano, J. M. (2018). Growth delay by winter precipitation could hinder *Juniperus sabina* persistence under increasing summer drought. *Dendrochronologia 51*, 22–31. https://doi.org/10.1016/j.dendro.2018.07.003

Gou, X., Gao, L., Deng, Y., Chen, F., Yang, M., & Still, C. (2015). An 850-year tree-ring-based reconstruction of drought history in the western Qilian Mountains of northwestern China. *International Journal of Climatology 35* (11), 3308–3319. https://doi.org/10.1002/joc.4208

Grießinger, J., Bräuning, A., Helle, G., Thomas, A., & Schleser, G. (2011) Late Holocene Asian summer monsoon variability reflected by $\delta^{18}O$ in tree-rings from Tibetan junipers. *Geophysical Research Letters 38* (3), L03701. https://doi.org/10.1029/2010GL045988

Hantemirov, R. M., Gorlanova, L. A., & Shiyatov, S. G. (2004). Extreme temperature events in summer in northwest Siberia since AD 742 inferred from tree rings. *Palaeogeography Palaeoclimatology Palaeoecology 209* (1–4), 155–164.

https://doi.org/10.1016/j.palaeo.2003.12.023

Holmes, R. L. (1983). Computer-assisted quality control in tree-ring dating and measurement. *Tree-Ring Bulletin 1983*, 69–78.

Li, R., Luo, T., Molg, T., Zhao, J., Li, X., Cui, X., et al. (2016). Leaf unfolding of Tibetan alpine meadows captures the arrival of monsoon rainfall. *Scientific Reports 6*, 20985. https://doi.org/10.1038/srep20985

Liang, E., Lu, X., Ren, P., Li, X., Zhu, L., & Eckstein, D. (2012). Annual increments of juniper dwarf shrubs above the tree line on the central Tibetan Plateau: a useful climatic proxy. *Annals of Botany 109* (4), 721–728. https:// doi.org/10.1093/aob/mcr315

Liang, E., Dawadi, B., Pederson, N., Piao, S., Zhu, H., Sigdel, S. R., et al. (2019). Strong link between large tropical volcanic eruptions and severe droughts prior to monsoon in the central Himalayas revealed by tree-ring records. *Science Bulletin 64* (14), 1018–1023. https://doi.org/10.1016/j.scib.2019.05.002

Lin, Z., & Wu, X. (1986). A preliminary analysis of the regularity in flood, drought and snow storm in Tibetan Plateau during historical times (in Chinese). *Acta Meteorologica Sinica 44* (3), 257−264.

Liu, Y., Song, H., Sun, C., Song, Y., Cai, Q., Liu, R., et al. (2019). The 600-mm precipitation isoline distinguishes tree-ring-width responses to climate in China. *National Science Review 6* (2), 359–368. https://doi.org/10.1093/nsr/nwy101

Michaelsen, J. (1987). Cross-validation in statistical climate forecast models. *Journal of Climate and Applied Meteorology 26* (11), 1589–1600.

Piao, S., Wang, X., Park, T., Chen, C., Lian, X., He, Y., et al. (2020). Characteristics, drivers and feedbacks of global greening. *Nature Reviews Earth & Environment 1*, 14–27. https://doi.org/10.1038/s43017-019-0001-x

Ren, P., Rossi, S., Camarero, J. J., Ellison, A. M., Liang, E., & Peñuelas, J. (2018). Critical temperature and precipitation thresholds for the onset of xylogenesis of *Juniperus przewalskii* in a semi-arid area of the north-eastern Tibetan Plateau. *Annals of Botany 121* (4), 617–624. https://doi.org/10.1093/aob/mcx188

Sanmiguel-Vallelado, A., Camarero, J. J., Gazol, A., Morán-Tejeda, E., Sangüesa-Barreda, G.,

Alonso-González, E., et al. (2019). Detecting snow-related signals in radial growth of *Pinus uncinata* mountain forests. *Dendrochronologia 57,* 125622. https://doi.org/10.1016/j.dendro.2019.125622

Savitzky, A., & Golay, M. J. E. (1964). Smoothing and differentiation of data by simplified least squares procedures. *Analytical Chemistry 36*, 1627.

Schweingruber, F., & Poschlod, P. (2005). Growth rings in herbs and shrubs: life span, age determination and stem anatomy. *Forest Snow & Landscape Research 79* (3), 195–415.

Shao, X., Xu, Y., Yin, Z., Liang, E., Zhu, H., & Wang, S. (2010). Climatic implications of a 3585-year tree-ring width chronology from the northeastern Qinghai-Tibetan Plateau. *Quaternary Science Reviews 29* (17–18), 2111–2122. https://doi.org/10.1016/j.quascirev.2010.05.005

Shen, M., Piao, S., Cong, N., Zhang, G., & Janssens, I. A. (2015). Precipitation impacts on vegetation spring phenology on the Tibetan Plateau. *Global Change Biology 21* (10), 3647–3656. https://doi.org/10.1111/gcb.12961

Shi, X., Qin, N., Shao, X., Wang, Q., Zhu, X., & Zhu, H. (2009). The drought and flood signals in recent 700 years indicated by long tree-rings of *Sabina tibetica* in Zaduo of Qinghai Province (in Chinese). *Plateau Meteorology 28* (4), 769–776.

Trouet, V., & Oldenborgh, G. J. V. (2013). Knmi climate explorer: a web-based research tool for high-resolution paleoclimatology. *Tree-Ring Research 69* (1), 3–13. https://doi.org/10.3959/1536-1098-69.1.3

Vicente-Serrano, S. M., Beguería, S., & López-Moreno, J. I. (2010). A multiscalar drought index sensitive to global warming: the standardized precipitation evapotranspiration index. *Journal of Climate 23*, 1696–1718. https://doi.org/10.1175/2009JCLI2909.1

Wells. N., Goddard, S., & Hayes, M. J. (2004). A self-calibrating Palmer Drought Severity Index. *Journal of Climate 17*, 2335–2351 https://doi.org/10.1175/1520-0442(2004)017<2335:ASPDSI>2.0.CO;2

Wernicke, J., Stark, G., Wang, L., Grießinger, J., & Bräuning, A. (2019). Air moisture signals in a stable oxygen isotope chronology of dwarf shrubs from the central Tibetan Plateau. *Annals of Botany 124* (1), 53–64. https://doi.org/10.1093/aob/mcz030

Wigley, T. M. L., Briffa, K. R., & Jones, P. D. (1984). On the average value of correlated time series, with applications in dendroclimatology and hydrometeorology. *Journal of Climate and Applied Meteorology 23* (2), 201–213.

Wrozyna, C., Frenzel, P., Steeb, P., Zhu, L., Geldern, R., Mackensen, A., et al. (2010). Stable isotope and ostracode species assemblage evidence for lake level changes of Nam Co, southern Tibet, during the past 600 years. *Quaternary International 212* (1), 2–13. https://doi.org/10.1016/j.quaint.2008.12.010

Xiao, S., Ding, A., Tian, Q., Han, C., & Peng, X. (2019). Site-and species-specific climatic responses of two co-occurring shrubs in the temperate Alxa Desert Plateau, Northwest China. *Science of the Total Environment 667*, 77–85. https://doi.org/10.1016/j.scitotenv.2019.02.217

Yao, T., Duan, K., Xu, B., Wang, N., Guo, X., & Yang X. (2008). Precipitation record since AD 1600 from ice cores on the central Tibetan Plateau. *Climate of the Past 4*, 175–180. https://doi.org/10.5194/cp-4-175-2008

Yao, T., Xue, Y., Chen, D., Chen, F., Thompson, L., Cui, P., et al. (2019). Recent third pole's rapid warming accompanies cryospheric melt and water cycle intensification and interactions between monsoon and environment: multidisciplinary approach with observations, modeling, and analysis. *Bulletin of the American Meteorological Society 100*, 423–444. https://doi.org/10.1175/BAMS-D-17-0057.1

Yang, B., Wang, J., & Liu, J. (2019). A 1556 year-long early summer moisture reconstruction for the Hexi Corridor, Northwestern China. *Science China Earth Sciences 62* (6), 953–963. https://doi.org/10.1007/s11430-018-9327-1

Zhang, B., Zhao, X., Jin, J., & Wu, P. (2015). Development and evaluation of a physically based multiscalar drought index: The Standardized Moisture Anomaly Index. *Journal of Geophysical Research-Atmospheres 120* (22), 11575–11588. https://doi.org/10.1002/2015JD023772

Zhang, B., Xia, Y., Huning, L. S., Wei, J., Wang, G., & AghaKouchak, A. (2019). A framework for global multicategory and multiscalar drought characterization accounting for snow processes. *Water Resources Research 55* (11), 9258–9278.

https://doi.org/10.1029/2019WR025529

Zhang, Q., Evans, M. N., & Lyu, L. (2015). Moisture dipole over the Tibetan Plateau during the past five and a half centuries. *Nature Communications 6*, 8062. https://doi.org/10.1038/ncomms9062

Zhu, L., Lü, X., Wang, J., Peng, P., Kasper, P., Daut, G., et al. (2015). Climate change on the Tibetan Plateau in response to shifing atmospheric circulation since the LGM. *Scientific Reports 5*, 13318. https://doi.org/10.1038/srep13318

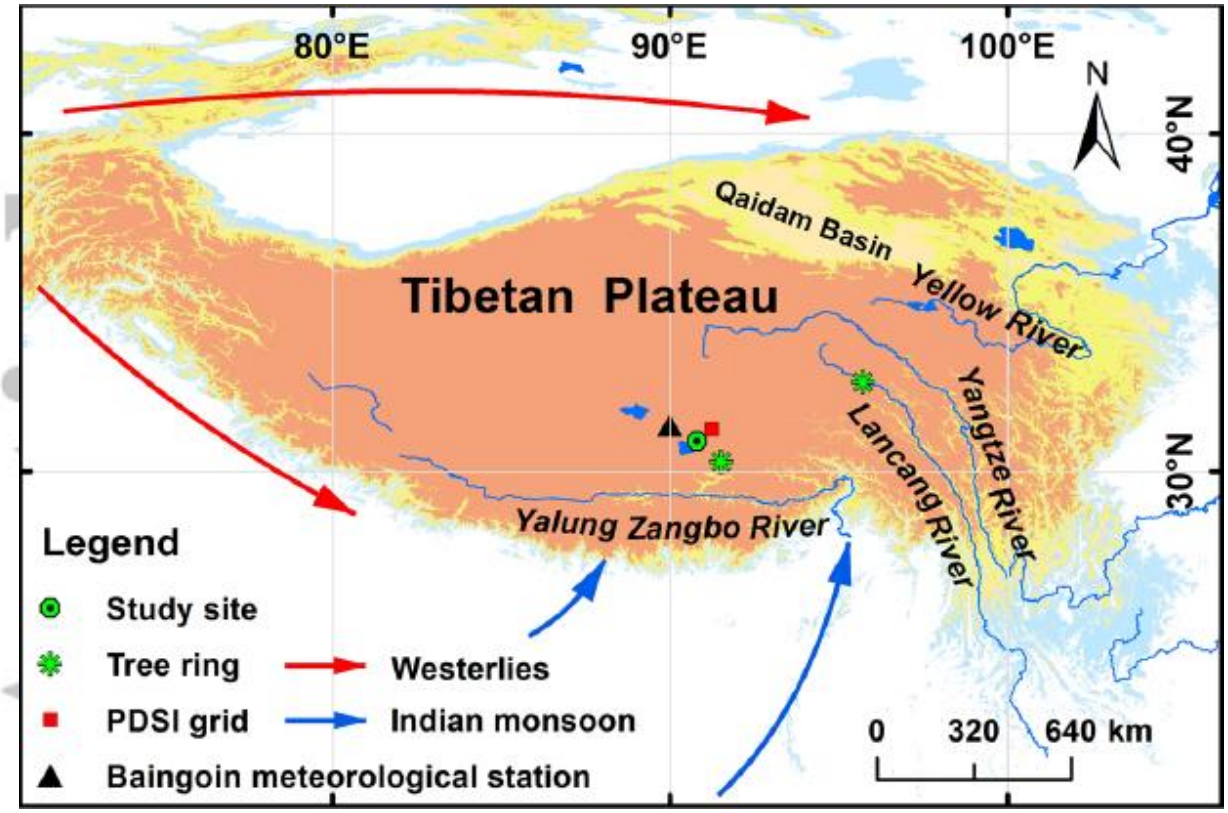

Figure 1. Locations of study site (green circle with dot) and Baingoin meteorological station (black triangle) on the southern Tibetan Plateau. The green asterisks correspond to the precipitation and drought reconstructions from tree-ring sites (Reting and Zaduo). The red box indicates the center of the 0.5° grid where the Palmer Drought Severity Index (PDSI) was reconstructed by Cook et al. (2010).

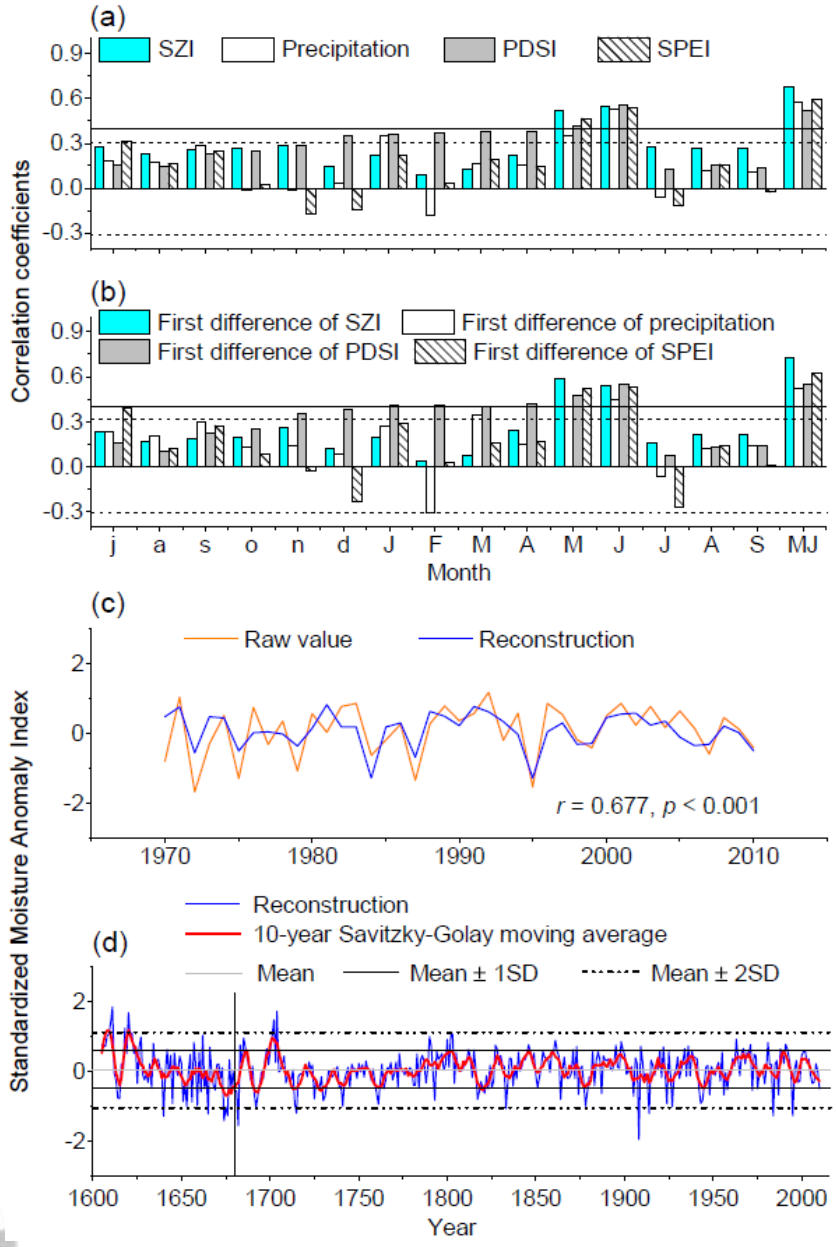

Figure 2. Pearson correlations (n = 41 years, period 1970–2010) between the ring-width chronology and SZI (5-month scale), precipitation, PDSI and SPEI (1-month scale) from previous July to current September (a) as well as for May-June (MJ) of the current year. Pearson correlations between the first differences of chronology and the above climate variables (b). The months of the previous and current years were indicated in lower-case and capital letters, respectively. The horizontal continuous and dashed lines represent the significance levels of 0.01 and 0.05, respectively (a, b). Observed raw (orange line) and reconstructed (blue line) May-June SZI values (c). May-June SZI (blue line) reconstruction and its 10-year moving average (red line) for the period of 1605–2010 (d). Mean value and standard deviations from the mean (± 1SD and ± 2SD) of reconstructed SZI are also shown (d). The black vertical line indicates the 1680 when the EPS value exceeds the threshold of 0.85 (see Figure S1).

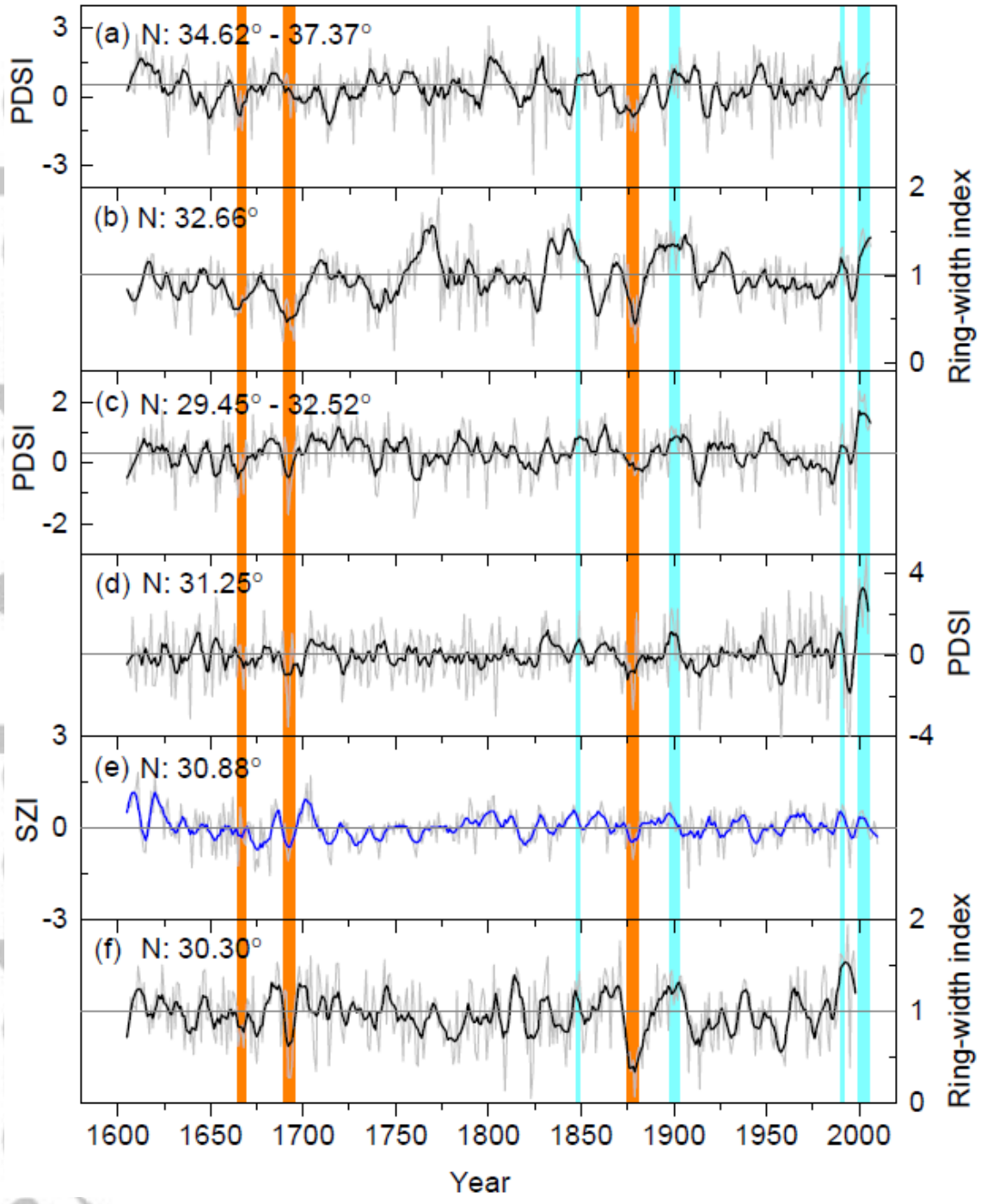

Figure 3. May-June PDSI reconstruction for the northern and southern Tibetan Plateau (Zhang, Evans, et al., 2015, a, c). Ring-width chronology used for May-June drought reconstruction in Zaduo County (Shi et al., 2009, b). Gridded PDSI reconstruction of June to August in the 0.5° grid located near the study site (Cook et al., 2010, d). May-June SZI reconstruction (this study, e). Ring-width index used for pre-monsoon rainfall reconstruction in Reting site (Bräuning & Grießinger, 2006, f). Low frequency variations of climate reconstructions in this and other studies are shown in blue and black lines, respectively. Orange and light cyan boxes indicate coincident dry and wet periods in low-frequency variance between the presented reconstructions, respectively.